European Journal of Medicinal Chemistry 54 (2012) 660–668

Contents lists available at SciVerse ScienceDirect

European Journal of Medicinal Chemistry

journal homepage: http://www.elsevier.com/locate/ejmech

Original article

Detailed structure–activity relationship of indolecarboxamides as H_4 receptor ligands

Harald Engelhardt [a,b], Iwan J.P. de Esch [b], Daniel Kuhn [a], Rogier A. Smits [b,c], Obbe P. Zuiderveld [b], Julia Dobler [a], Moriz Mayer [a], Sebastian Lips [a], Heribert Arnhof [a], Dirk Scharn [a], Eric E.J. Haaksma [a,b], Rob Leurs [b,*]

[a] Boehringer Ingelheim RCV GmbH & Co KG, Department of Medicinal Chemistry, Dr. Boehringergasse 5-11, Vienna, Austria
[b] Leiden/Amsterdam Center for Drug Research (LACDR), Division of Medicinal Chemistry, Department of Pharmacochemistry, Faculty of Sciences, VU University Amsterdam, De Boelelaan 1083, 1081 HV Amsterdam, The Netherlands
[c] Griffin Discoveries B.V., Department of Medicinal Chemistry, De Boelelaan 1083, 1081 HV Amsterdam, The Netherlands

ARTICLE INFO

Article history:
Received 16 March 2012
Received in revised form
5 June 2012
Accepted 9 June 2012
Available online 18 June 2012

Keywords:
Indolecarboxamide
Intramolecular Heck reaction
Histamine H_4 receptor (H_4R)
QSAR

ABSTRACT

A series of 76 derivatives of the indolecarboxamide **1** were synthesized, which allows a detailed SAR investigation of this well known scaffold. The data enable the definition of a predictive QSAR model which identifies several compounds with an activity comparable to **1**. A selection of these new H_4R antagonists was synthesized and a comparison of predicted and measured values demonstrates the robustness of the model (**47**–**55**). In addition to the H_4-receptor activity general CMC and DMPK properties were investigated. Some of the new analogs are not only excellently soluble, but display a significantly increased half-life in mouse liver microsomes as well. These properties qualify these compounds as a possible new standard for future in vivo studies (e.g **51**, **52** and **55**). Moreover, the current studies also provide valuable information on the potential receptor ligand interactions between the indolcarboxamides and the H_4R protein.

1. Introduction

Currently, four histamine receptors are known, namely the histamine H_1, H_2, H_3 and H_4 receptors. Bioinformatic analysis of the human genome database enabled the discovery of the H_4 receptor (H_4R) in the year 2000 [1–3]. The H_4R belongs to the GPCR gene family. Initially, the expression of the H_4R was thought to mainly occur in the periphery on dendritic cells, mast cells, eosinophils, monocytes, basophils, natural killer cells, and T cells[4,5]. Recent studies however, also revealed its presence in several regions of the CNS [6,7]. Meanwhile there is clear evidence, based on animal models, that the H_4R plays a role in immune and inflammatory responses [4] and modulates itch responses as well [8–10]. It has been reported that antagonists of the H_4R are able to block the shape change and chemotaxis of eosinophils and mast cells, which are involved in modulating many inflammatory processes [11,12]. These findings suggest that H_4R antagonists could play a role in e.g. the treatment of asthma and rheumatoid arthritis [13]. The H_4R research field was given an important boost by the discovery and early disclosure of the antagonist H_4R antagonist JNJ7777120 **1** (Fig. 1) by Carruthers et al. [14–16]. This indolecarboxamide-containing ligand is a potent and selective H_4R antagonist and, importantly, was the first antagonist to be devoid of H_1R–H_3R activity [14,15]. Several other H_4R antagonists have been published in the meanwhile by various labs [20–23], but **1** is still the best studied H_4R compound for which a large number of in vitro and in vivo studies have been shown. It inhibits human eosinophil and murine bone-marrow mast cell chemotaxis with IC_{50} values of 86 nM and 40 nM, respectively [22]. The administration of **1** also significantly reduced inflammatory indicators in a murine model of asthma [22]. A drawback of this H_4R antagonist is however its short half-life in rodents which most likely hampers further development and detailed pharmacological studies. The critical PK property can be attributed to its low stability in mouse and rat liver microsomes [20]. In depth analysis of mice PK experiments have shown that the demethylated compound **2** is the most prominent metabolite of **1** [20]. As compound **2** is still a potent H_4R antagonist it is at this moment unclear to what extent metabolite **2** contributes to the observed *in vivo* activities.

Compound **1** and derivatives have also been instrumentals in the construction of various pharmacophore models, homology

* Corresponding author. Tel.: +31 (0)205987600; fax: +31 (0)205987610.
E-mail address: r.leurs@vu.nl (R. Leurs).

0223-5234/$ – see front matter © 2012 Elsevier Masson SAS. All rights reserved.
http://dx.doi.org/10.1016/j.ejmech.2012.06.016

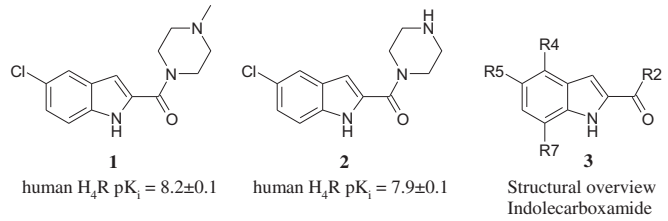

Fig. 1. Structure and activity of **1** and its main metabolite; structural overview of indolecarboxamides.

models and rough QSAR models [17–19], that enabled virtual screening [24], fragment-based approaches and scaffold hopping in order to derive new compound classes. For some of these new H_4R classes (e.g., containing pyrimidine, quinazoline and quinoxaline scaffolds) extensive SAR explorations have been published [20–22].

The available data for the indolecarboxamide scaffold indicate that at position R2, R4, R5 and R7 several different substituents are tolerated with respect to H_4R activity (see Fig. 1) [14,15]. Unfortunately, so far only a limited number of substitution patterns have been published at these four positions. In order to aid detailed understanding of the receptor–ligand interactions at the human H_4R and enable comparison with the above mentioned compound classes, we set out to generate a comprehensive SAR for the indolecarboxamide scaffold and study these relationships in a more quantitative manner using a predictive Free-Wilson QSAR model [25]. This model was subsequently used for the identification of indolecarboxamides, which display at least a comparable H_4R affinity to **1**.

2. Results and discussion

2.1. Chemistry

Starting from hydrazines **4a**–**4e** the acids **5a**–**5e** bearing a x_7 substituent (x_7 = C-R7; R7 ≠ H) were synthesized via Fisher indole synthesis, as in these cases the reaction results in the required regioisomer (see Scheme 1). The intramolecular Heck reaction starting from halogenanilines **4f**–**4h** was used for acids **5f**–**5h**, as this type of reaction results directly in the desired regioisomer (see Scheme 1). All other acids (**5i**–**5af**) are commercially available.

The central step in synthesis of the final compounds was an amide coupling starting from acids **5a**–**5af** and commercially available diamines **6a**–**6g** (see Scheme 1, Table 1 and Scheme 2).

The acids **5a**–**5af** were activated using 2-(7-aza-1*H*-benzotriazole-1-yl)-1,1,3,3-tetramethyluronium hexafluorophosphate and N,N-diisopropylethylamine. The active esters were treated with the corresponding amines **6a**–**6g**, which led to the desired amides **1**–**79** (see Scheme 2) (Table 2).

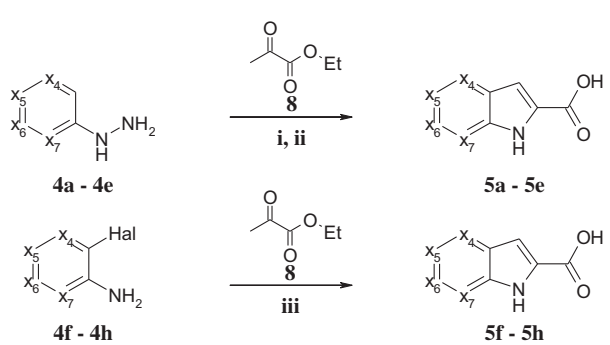

Scheme 1. Reagents and conditions: (i) toluene-4-sulfonic acid, toluene, reflux, 14–24 h; (ii) 1. toluene-4-sulfonic acid, toluene, reflux, 1 h; 2. polyphosphor acid, 195 °C, 5–10 min; (iii) 1. pyridinium p-toluenesulfonate, tetraethoxy-silane, pyridine, 20 °C, 24 h; 2. $Pd[P(C_6H_6)_3]_4$, N,N-dicyclohexylmethylamine, 160 °C, 20 min.

Table 1
Acids **5a**–**5af**.

#	x1	x4	x5	x6	x7
5a	NH	CH	CCl	CH	CF
5b	NH	CH	CCl	CH	CCH_3
5c	NH	CH	CCl	CH	CNO_2
5d	NH	CF	CH	CH	CCH_3
5e	NH	CF	CH	CH	CF
5f	NH	N	CH	CH	CH
5g	NH	CH	CH	N	CH
5h	NH	$CCOCH_3$	CH	CH	CH
5i	NH	CH	CCl	CH	CH
5j	NH	CH	CH	CH	CH
5k	S	CH	CH	CH	CH
5l	O	CH	CCl	CH	CH
5m	NH	CH	N	CH	CH
5n	NH	CH	CH	CH	N
5o	NH	CF	CH	CH	CH
5p	NH	CCl	CH	CH	CH
5q	NH	$COCH_3$	CH	CH	CH
5r	NH	CNO_2	CH	CH	CH
5s	NH	CH	$COCH_3$	CH	CH
5t	NH	CH	CNO_2	CH	CH
5u	NH	CH	$CCOCH_3$	CH	CH
5v	NH	CH	CH	CCl	CH
5w	NH	CH	CH	$COCH_3$	CH
5x	NH	CH	CH	CNO_2	CH
5y	NH	CH	CH	CH	CF
5z	NH	CH	CH	CH	CCH_3
5aa	NH	CH	CH	CH	$COCH_3$
5ab	NH	CH	CH	CH	CNO_2
5ac	NH	CH	CH	CH	CCF_3
5ad	NH	CH	CH	CH	CCH_3
5ae	NH	CF	CCl	CH	CH
5af	NH	CCl	CCl	CH	CH

In several cases the amide was further manipulated. For example the Boc-protection group was removed (compounds **2a** → **2**, **43a** → **43**, **44a** → **44**, **45a** → **45**, **52a** → **52**, **53a** → **53**, **54a** → **54**, **64a** → **64**, **65a** → **65**, **66a** → **66**, **68a** → **68**, **72a** → **72**, **73a** → **73**, **74a** → **74**, Scheme 2), a nitro group was reduced (compounds **21** → **22**, **28** → **29**, **34** → **35**, **40** → **41**, **75** → **51**, Scheme 2) or a methoxy group (compound **19** → **20**) was demethylated.

2.2. In vitro studies

2.2.1. H_4R radioligand displacement assay

The affinity of the various compounds was determined by the displacement of [3H]histamine binding the human H_4R as described previously [19]. The given pK_i values are mean values ± SEM of at least three independent determinations.

Table 2
Diamines **6a**–**6g**.

#	Structure	#	Structure	#	Structure
6a	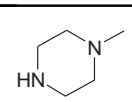	**6d**	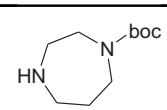	**6f**	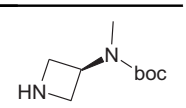
6b	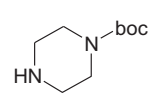	**6e**	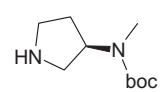	**6g**	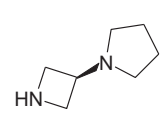
6c	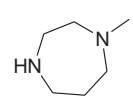				

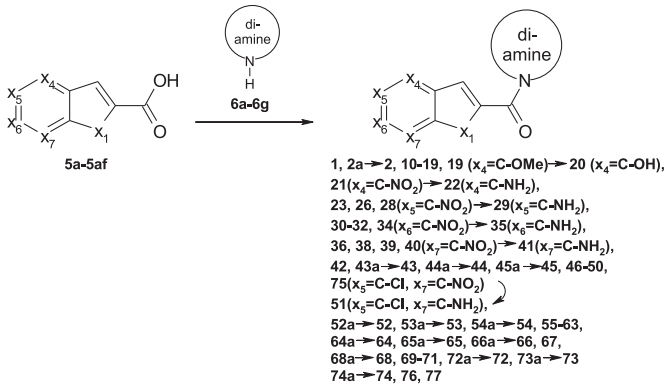

Scheme 2. Reagents and conditions: 2-(7-Aza-1*H*-benzotriazole-1-yl)-1,1,3,3-tetramethyluronium hexafluorophosphate, N,N-diisopropylethylamine, N,N-dimethylformamide, 20 °C, 1–16 h.

2.2.2. Determination of solubility

Solubility measurements were performed by DMSO solution precipitation. This methodology is in line with the method described by K. Sugano et al. [26].

2.2.3. Microsomal stability assay

Liver microsomes were purchased from Xenotech and the stability assay for the determination of $t_{1/2}$ was performed as described in a publication from S.M. Skaggs et al. [27].

2.3. Computational methods

The Free-Wilson analysis was performed using the statistic software package R [28]. A R-group decomposition was performed using Pipeline Pilot [29]. Presence and absence of functional groups was encoded in a binary fingerprint for each compound. Using the lm function (function in software package R [28] for linear regression calculation) a linear regression model was constructed.

2.4. SAR discussion

2.4.1. SAR of indole replacements

In a first step the direct modification of the indole scaffold was investigated. The indole moiety was replaced by other heteroaromatic systems. It has been published, that thienopyrroles and benzimidazoles are alternatives for the indole moiety [15]. Compounds bearing such residues display a comparable H_4R affinity to **1**, but show even less attractive DMPK properties [15,22]. Compound **11** and **12** (Table 3), the benzthieno and benzfuro analog of **10** and **1**, display a 100 fold decreased H_4R affinity, illustrating clearly that the NH-donor of the indole scaffold is essential for a good H_4R interaction (Table 4).

In a next step the benzene ring of the indole **10** was replaced by pyridines. All four possible pyridine analogs **13**–**16** of indole **10** display a significant drop in H_4R affinity (Table 3). This indicates that electron-poor ring systems are not tolerated. This is in line with previous SAR studies which have shown that the benzene portion of the indole **10** can be replaced by the electron-rich thiophene [15].

These data also clearly demonstrate that in the current series the indole ring is the optimal scaffold for H_4R-antagonists. Therefore an extensive series of ring substitutions on this scaffold were prepared in the next step (Table 5).

2.4.2. SAR of different substitution patterns on the indole scaffold

Substitution of the benzene portion of the indole scaffold was investigated and the resulting affinities compared to the unsubstituted indolecarboxamide **10**, which possesses a pK_i on the human H_4R receptor of 7.6 ± 0.1.

Lipophilic groups like fluorine, chlorine or methyl are tolerated at all positions and result in compounds (**1**, **17**, **18**, **24**, **25**, **31**, **36**, **37**, **38**) which show comparable affinity or as in case of **1** an improved affinity compared to the unsubstitued indole **10**. The exception is position R6, where introduction of a chlorine atom causes a significant drop in activity (compound **31**; H_4R $pK_i = 6.9 \pm 0.1$). The affinity of the fluorine substituted indoles **24** and **36** is comparable to the methyl substituted indoles **25** and **38**. This indicates that the electronic properties of the lipophilic substituents do not have

Table 3
Human H_4R binding affinity of indolecarboxamide analogs.

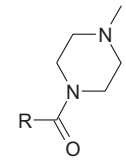

#	R-group	hH_4R $pK_i \pm SEM$	#	R-group	hH_4R $pK_i \pm SEM$
10	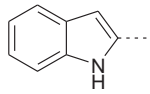	7.6 ± 0.1	**13**	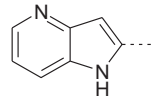	5.4 ± 0.1
1	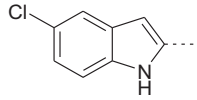	8.2 ± 0.1	**14**	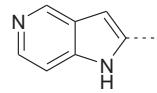	5.2 ± 0.1
11	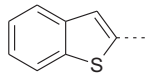	5.6 ± 0.1	**15**	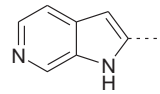	5.7 ± 0.1
12	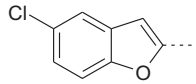	6.6 ± 0.1	**16**	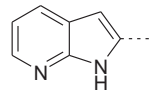	5.7 ± 0.1

Table 4
Binding affinity of R4, R5, R6 or R7 mono-substituted indolecarboxamides.

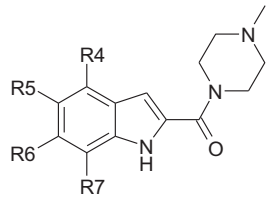

.

R-groups	#	R4 hH_4R $pK_i \pm SEM$	#	R5 hH_4R $pK_i \pm SEM$	#	R6 hH_4R $pK_i \pm SEM$	#	R7 hH_4R $pK_i \pm SEM$
H	**10**	7.6 ± 0.1	**10**	7.6 ± 0.1	**10**	7.6 ± 0.1	**10**	7.6 ± 0.1
F	**17**	7.5 ± 0.1	**24**	7.8 ± 0.1[a]		–	**36**	7.7 ± 0.1
Cl	**18**	7.5 ± 0.1	**1**	8.2 ± 0.1	**31**	6.8 ± 0.1	**37**	7.7 ± 0.1[a]
Me		–	**25**	7.3 ± 0.1[a]		–	**38**	7.9 ± 0.1
OMe	**19**	6.0 ± 0.1	**26**	6.0 ± 0.1	**32**	4.8 ± 0.1	**39**	5.6 ± 0.1
OH	**20**	6.8 ± 0.1	**27**	7.6 ± 0.1[a]	**33**	7.6 ± 0.1		–
NO_2	**21**	6.1 ± 0.1	**28**	7.1 ± 0.1	**34**	5.7 ± 0.1	**40**	6.1 ± 0.1
NH_2	**22**	6.5 ± 0.1	**29**	7.5 ± 0.1	**35**	7.1 ± 0.1	**41**	7.8 ± 0.1
COMe	**23**	5.3 ± 0.1	**30**	4.9 ± 0.1		–		–
CF_3		–		–		–	**42**	6.0 ± 0.1

[a] Data from Refs. [14] and [15].

Table 5
Binding affinity of indolecarboxamides bearing different cyclic diamines.

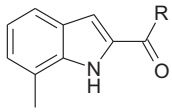

.

#	R-group	hH4R $pK_i \pm SEM$	#	R-group	hH4R $pK_i \pm SEM$
38	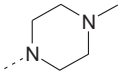	7.9 ± 0.1	**45**	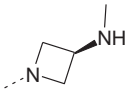	6.4 ± 0.1
43	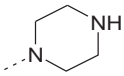	7.4 ± 0.1	**46**	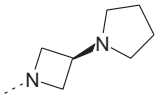	7.1 ± 0.1
44	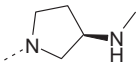	6.2 ± 0.1			

a strong influence on the H_4R affinity. This is in contrast to the aza-indoles **13**–**16**, where the electronic poor ring system leads to a clearly decreased H_4R affinity. We therefore hypothesize that the unfavorable electronic withdrawing property of the fluorine moiety is compensated through a strongly positive lipophilic interaction with the H_4R protein.

Indoles with methoxy substituents (**19**, **26**, **32** and **39**) show a significantly decreased H_4R affinity when compared to the unsubstituted indole **10**. As electronic properties are of minor relevance for H_4R affinity, the reduction in affinity is most likely caused by the difference in steric properties. This hypothesis is further supported by indoles bearing electron-withdrawing groups, like a nitro (**21**, **28**, **34** and **40**) or a CF_3 moiety (**42**), which display a similar size as the methoxy group.

Compounds substituted with a nitro group (**21**, **28**, **34** and **40**) are less active than reference compound **10**. The exception is 5-nitro-indole **28**, where a larger residue is tolerated and only a slight decrease in affinity is observed. A favorable interaction of the oxygen atoms of the nitro group with the H_4R could be the reason for the difference to 5-methoxy-indole **26**. Also, the electron-withdrawing 7-trifluoromethyl-indole **42** and both methylketone substituted indoles **23** and **30** show a significantly decreased H_4R activity in comparison to **10**.

Indoles with small polar groups like an amino or a hydroxyl group at position R5, R6 and R7 (**27**, **29**, **33**, **35** and **41**) display a comparable H_4R affinity to the unsubstituted indole **10**. However, substitution at the R4 position with those polar substituents lead to compounds (**20** and **22**) with strongly decreased H_4R affinity in comparison to reference compound **10**, suggesting a small lipophilic pocket in this region of the receptor.

In summary, at position R4 only small lipophilic substituents are tolerated. Position R5 and R7 can be substituted with small lipophilic and small polar groups without losing activity. At position R6 only small polar groups are tolerated.

2.4.3. SAR of the basic side chain – position R2

About the SAR of position R2, the basic side chain/subsituent, only little is known, although for other H_4R classes extensive series exploring alternative basic groups to replace the methyl-piperazine have been described [14,20,21]. We therefore prepared a series of cyclic diamines, where the basic center is in a similar region as piperazine. These investigations were done on the 7-methyl-indolecarboxamide scaffold, as **38** was shown to be one of the most active derivatives (see Table 3).

Changing the R2 substituent from 4-methyl-piperazine to an unsubstituted piperazine reduces the affinity of the resulting compound **43,** by a factor of 3. The 3-aminomethyl-pyrrolidine and the 3-aminomethyl-azetidine substituted indolecarboxamide **44** and **45** display a pK_i on H_4R of around 6. Interestingly, the increase in lipophilicity at the azetidine leads to compound **46** with an improved affinity (H_4R $pK_i = 7.1 \pm 0.1$) compared to compound **45**. Compound **46** has a reduced affinity of a factor of 7 in comparison to the methylpiperazine analog **38**.

2.5. Generation of a quantitative QSAR model

2.5.1. Establishment and validation of a Free-Wilson model

The theoretical number of combinations of the substituents described above would give rise to a library of compounds of 21,504 members. In order to efficiently select the most attractive combinations we used the 41 synthesized indolecarboxamides (compounds **1**, **2**, **10**, **17**–**23**, **26**, **28**–**32**, **34**–**36**, **38**–**46**, and **56**–**68** from Supplementary Table 1) to build a QSAR model based on a Free-Wilson analysis.

The Free-Wilson analysis is a simple method that aims for a quantitative SAR description of a given compound series. It relates, via indicator variables, the presence or absence of functional groups with biological activity. Multiple linear regression methods were used to derive an equation, which was subsequently used to predict novel compounds. The 41 indolecarboxamides (compounds **1**, **2**, **10**, **17**–**23**, **26**, **28**–**32**, **34**–**36**, **38**–**46**, and **56**–**68** from Supplementary Table 1), which were used to build the model, share the indole moiety as core structure and are substituted in one of the R2, R4, R5, R6, and R7 positions. The derived model was used to predict the activity of novel tri-substituted compounds.

The Free-Wilson model shows an excellent fit of the experimental data (adjusted $r^2 = 0.90$). Eq. (1) lists the obtained Free-Wilson equation, which was used for further analysis. Summary statistics can be found in the Supplementary Table 3.

$$\begin{aligned} pK_{ipred} = {} & 6.427 + 1.101\ \mathrm{CN1CCN(CC1)C(=O)[R2]} \\ & - 0.748\ \mathrm{O[R4]} + 0.735\ \mathrm{Cl[R5]} - 1.528\ \mathrm{CO[R4]} \\ & - 1.777\ \mathrm{CO[R7]} - 0.055\ \mathrm{C[R7]} \\ & - 1.478\ \mathrm{[O-][N+](=O)[R7]} - 1.508\ \mathrm{CO[R5]} \\ & - 0.438\ \mathrm{[O-][N+](=O)[R5]} + 0.073\ \mathrm{F[R4]} \\ & - 0.184\ \mathrm{CN[C@@H]1CCN(C1)C(O=)[R2]} + 0.771\ \mathrm{O} \\ = {} & \mathrm{C(N1CCNCC1)[R2]} - 0.468\ \mathrm{N[R6]} - 2.228\ \mathrm{CC(=O)[R4]} \\ & - 2.618\ \mathrm{CC(=O)[R5]} + 0.232\ \mathrm{N[R7]} + 0.831\ \mathrm{O} \\ = {} & \mathrm{C(N1CC(C1)N2CCCC2)[R2]} - 1.377\ \mathrm{FC(F)(F)[R7]} \\ & - 0.068\ \mathrm{N[R5]} - 2.698\ \mathrm{CO[R6]} - 0.688\ \mathrm{Cl[R6]} \\ & - 0.988\ \mathrm{N[R4]} - 1.438\ \mathrm{[O-][N+](=O)[R4]} \\ & - 1.818\ \mathrm{[O-][N+](=O)[R6]} \end{aligned} \tag{1}$$

To assess the predictive power of the model a leave-one-out (LOO) and leave-one-group out cross-validation (e.g. by dividing the dataset into five parts) was performed. The five-fold cross-validation had a high prediction error of 0.93 (cross-validation estimate of prediction error). Close inspection of the training set compounds reveals imbalances in the dataset that lead to the poor internal cross-validation results. Many substituents were only present in one molecule (e.g. **26** methoxy in R5). If one of these

molecules was left out during cross-validation high prediction errors were obtained. Also removal of variables with one non-zero value did not improve the results.

To assess the risk of chance correlation, the affinity values were randomly scrambled and a linear regression analysis was performed, using 100 different randomization runs. The adjusted r^2 values served as criterion to determine the percentage of change correlations that were better than the Free-Wilson model based on the correct ordering of the affinity values. The distribution of the adjusted r^2 values was distinct from the model based on the correct affinities. No single y-scrambled model adjusted r^2 value was better than the presented Free-Wilson model based on correct affinities. To evaluate the predictive power of the y-scrambled models each model was used to predict the affinities of the external test set. The obtained predictive r^2 values (Supplementary Fig. 1) were clearly distinct from the real model with a predictive r^2 value of 0.90 (Fig. 2). This further underlines the fact that the applied Free-Wilson model is able to predict the affinity of novel compounds.

2.5.2. Prediction of new compounds using the Free-Wilson model

One prerequisite of a Free-Wilson analysis is additivity of the single R-groups. We tested this hypothesis by synthesizing and testing a subset of compounds. A set of compounds bearing two substituents at the phenyl part of the indolecarboxamide moiety was selected. It was further required that the selected compound should spread at least an affinity range of 2 log units. Our presumption was that the existing SAR information would be sufficient to design and enrich compounds that are more active than **10**.

Out of the chemical space of 21,504 theoretically possible compounds covered by the Free-Wilson model, 18 indolecarboxamides (compounds **47**–**55** and compounds **69**–**77** from Supplementary Table 2) were synthesized and tested for H_4R affinity. These compounds also served as the external test set in a cross-validation experiment. Fig. 2 shows the plot of the experimentally determined affinity against the predicted affinity. The predicted affinities are in good agreement with the experimentally determined binding affinities ($r^2 = 0.90$), showing that the Free-Wilson model is able to predict the affinities of new compounds.

The resulting Free-Wilson model provides the following overall information. A chloro-substituent in the R5-position or an amino residue in the position R7 shows a strong contribution to the high affinity (Eq. (1)). Especially the combination of a chloro-substituent in position R5 with halogens in position R4 (compound **47** and **48**) or fluoro-, methyl- or amino substituent in position R7 lead to highly active derivatives (compound **49**–**51**). Different R2 residues have a large influence on the binding affinity (see compound **50** and **52**–**55**). The most active compounds bearing a 4-methyl-piperazine, the corresponding 4-H-piperazine, or the 3-pyrrolidine-azetidine moiety in position R2 (e.g. **50**, **52** and **55**). All other investigated R-groups have a negative sign and do not contribute to binding (Eq. (1)). These findings suggest that on the basis of the model the most promising R-group combinations have been synthesized.

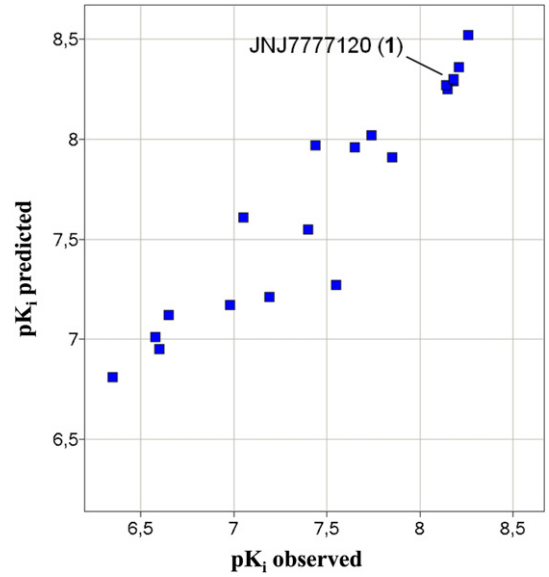

Fig. 2. Experimentally determined pK_i's vs. predicted pK_i's show good correlation ($r^2 = 0.90$). The JNJ777120 was not part of the external test set, but is shown for comparison.

2.6. Summary of SAR information

In Fig. 3 all collected SAR information is summarized. The different basic diamines investigated show clearly that proper placement and decoration of the positively charged amine is very important for high H_4R activity. For position X only NH leads to a high H_4R affinity indicating that the NH forms a H-bond to the GPCR protein. On position R4 only small halogens are tolerated, suggesting that the protein might have a small complementary lipophilic pocket. SAR investigation for the position R5 reveals that the H_4R protein presents in these regions amino acids which can form favorable interactions with lipophilic residues like halogens as well with polar moieties like amino or hydroxyl groups. The region around the position R6 seems to consist of polar amino acids, because at this position only polar groups are tolerated. The surrounding of position 7 seems to be quite similar to position 5, as there also lipophilic as well as polar moieties are tolerated.

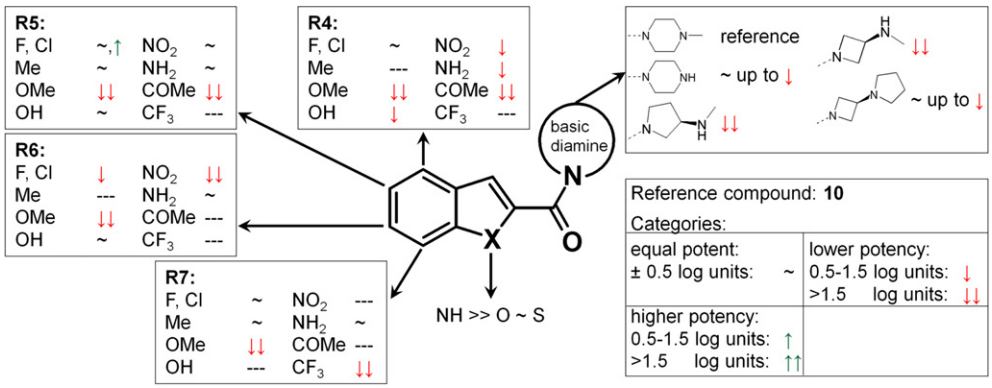

Fig. 3. SAR summary of indolecarboxamides.

2.7. Investigation of DMPK and CMC parameters

The indolecarboxamide **1** displays a clear metabolic liability in rodents (half live in mouse liver microsomes: 2 min). Metabolism studies have shown that the R2 methyl-piperazine moiety (see Fig. 1), is rapidly demethylated. Therefore, it was investigated whether the new indolecarboxamides **52**–**55**, bearing a different R2 substituent can overcome this issue (Table 6).

The methylpiperazine derivative **50** displays a similar short half life in mouse liver microsomes as **1** (Table 7). The demethylated compound **52** shows a 8-fold increased half life in mouse liver microsomes compared to **50**. Replacement of the methyl group in position 7 of compound **50** to a amino group leads also to a increased stability in mouse liver microsomes (**51**) and in addition the potency is even slightly increased with respect to **50**. The stability in mouse liver microsomes can be further increased by introduction of the 3-aminomethyl-pyrolidine (compound **53**) or the 3-aminomethyl-azetidine (compound **54**) moiety at position 2. With a 5 fold improved stability on mouse liver microsomes compared to **50**, compound **55** represents the best compromise between activity and stability. The solubility of compounds **52**–**55** at pH 6.8 is acceptable and should not be a limiting factor for a good in vivo exposure.

3. Conclusions

Generation of comprehensive SAR around the indolecarboxamide scaffold enables the establishment of a predictive QSAR model. This model predicts several compounds with an activity comparable to **1**. Several new H_4R antagonists were synthesized and the predicted and measured values correlate well. In addition, some of the new analogs display a significantly increased half-life in mouse liver microsomes. The good solubility at pH 6.8 qualifies these compounds for future in vivo studies (e.g compound **52** and **55**).

Using this strategy for optimization of the indolecarboxamide scaffold keeps the synthetic effort to a minimum and delivers a QSAR model, which can also used in further optimization cycles.

The current studies also provide valuable information on the potential receptor ligand interactions between the indolcarboxamides and the H_4R protein. This map will be used in a subsequent study to define a detailed 3-dimensional model of the current series with the H_4R. Comparing the SAR of different classes of H_4R ligands will give further insights in ligand recognition of the H_4R.

Table 6
Examples of predicted and experimentally determined binding affinity of indolecarboxamides.

	#	R-groups	Predicted hH_4R pK_i	hH_4R $pK_i \pm SEM$
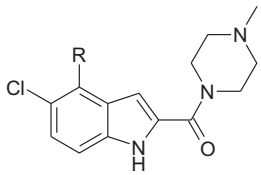	**47**	F	8.3	8.2 ± 0.1
	48	Cl	8.3	8.2 ± 0.1
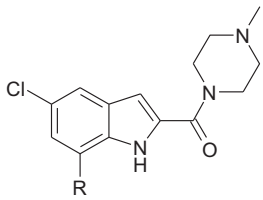	**49**	F	8.3	8.2 ± 0.1
	50	Me	8.3	8.2 ± 0.1
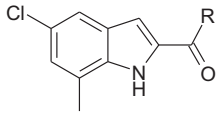	**51**	NH_2	8.5	8.3 ± 0.1
	50	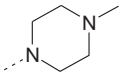	8.3	8.2 ± 0.1
	52	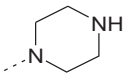	7.9	7.9 ± 0.1
	53	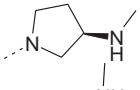	7.0	6.6 ± 0.1
	54	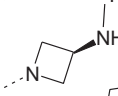	7.2	6.7 ± 0.1
	55	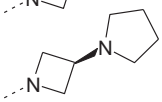	8.0	7.5 ± 0.1

Table 7
DMPK & CMC properties of indolecarboxamides

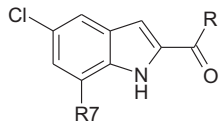

.

#	R-group	R 7-group	hH_4R $pK_i \pm SEM$	Half life in HLM [min]	Half life in MLM [min]	Solubility @ pH 6.8 [μg/ml]
50	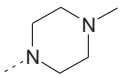	Me	8.2 ± 0.1	>45	2	57
51	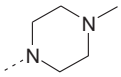	NH_2	8.3 ± 0.1	66	14	67
52	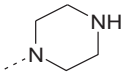	Me	7.9 ± 0.1	>90	16	65
53	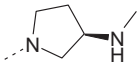	Me	6.6 ± 0.1	>90	27	59
54	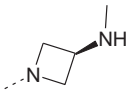	Me	6.7 ± 0.1	>90	26	51
55	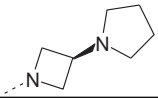	Me	7.5 ± 0.1	>90	11	10

4. Experimental procedures

4.1. General

Chemicals and reagents were obtained from commercial suppliers and were used without further purification. Proton and Carbon NMR spectra were obtained on a Bruker Advance 400 FT-NMR or Bruker Advance 500 FT-NMR instrument with chemical shifts (δ) reported relative to tetramethylsilane as an internal standard.

Analytical HPLC-MS analyses were conducted using an Agilent 1100 series LC/MSD system. The analytic method A1 is defined in Table 8. Compound purities were calculated as the percentage peak area of the analyzed compound by UV detection at 254 nm. If purity data is not explicitly mentioned the compound displays a purity >95%. Flash column chromatography was carried out using hand packed silica gel 60 (230–400 mesh) or pre-packed silica gel columns from Biotage and product was eluted under medium pressure liquid chromatography. Preparative high performance chromatography was carried out on a Gilson system (pump system: 333 & 334 prep-scale HPLC pump; fraction collector: 215 liquid handler; detector: Gilson UV/VIS 155) using pre-packed reversed phase silica gel columns from waters. The methods for preparative high performance chromatography P1–P3 are defined in Table 8. Thin-layer chromatography (TLC) was performed using 2.5 × 7.5 cm silica gel 60 glass-backed plates with a fluorescent (F254) indicator from Merck.

4.2. Synthesis of compounds

4.2.1. General method A – Fisher indole method for synthesis of indole carboxylic acids

*4.2.1.1. 5-Chloro-7-fluoro-1H-indole-2-carboxylic acid (**5a**).* (4-Chloro-2-fluoro-phenyl)hydrazine **4a** (1.00 g, 5.08 mmol), ethyl pyruvate **8** (0.56 ml, 5.08 mmol) and toluene-4-sulfonic acid monohydrate (23 mg, 0.12 mmol) were dissolved in 70 ml toluene and stirred under reflux conditions. After 2 h, additional toluene-4-sulfonic acid monohydrate (3.28, 17.26 mmol) was added and the mixture was refluxed for further 12 h. The reaction mixture was cooled down to 20 °C and diluted with 300 ml ethyl acetate and treated with 200 ml saturated sodium hydrogencarbonate solution. The organic layer was separated and treated three additional times with 200 ml saturated sodium hydrogencarbonate solution. The organic layer was dried with sodium sulfate, the solvent was evaporated under reduced pressure and the crude product was purified using chromatography method P1, yielding 288 mg (1.19 mmol) of (5-Chloro-7-fluoro-1*H*-indol-2-yl)-carboxylic acid ethyl ester. The ester was dissolved in 5 ml ethanol and 5 ml water. To this solution lithium hydroxide (240 mg, 10.00 mmol) was added. After 16 h the pH value of the reaction mixture was adjusted to pH 4 and ethyl acetate was added. The organic layer was separated and dried with sodium sulfate. The solvent was evaporated under reduced pressure, yielding 208 mg (19%) of the title compound. Purity by method A1: >95%; MS (ESI) *m/z* 214/216 $(M+H)^+$, Cl distribution; ^{1}H NMR (DMSO) δ (ppm) 12.48 (br, 1H), 7.60 (d, $J = 1.8$ Hz, 1H), 7.23 (dd, $J = 1.8$ Hz, $J_{HF} = 11.05$ Hz, 1H), 7.16 (dd, $J = 1.8$ Hz, $J = 3.2$ Hz, 1H).

*4.2.1.2. Indole carboxylic acids **5b**, **5d** and **5e**.* Indole carboxylic acids **5b**, **5d** and **5e** are synthesized in a similar manner to **5a**.

4.2.2. General method B – intramolecular heck method for the synthesis of indole carboxylic acids or pyrrolopyridine carboxylic acids

*4.2.2.1. 1H-Pyrrolo[3,2-b]pyridine-2-carboxylic acid (**5f**).* 3-Amino-2-chloro-pyridine **4f** (150 mg, 1.17 mmol), ethyl pyruvate **8** (0.25 ml, 2.00 mmol), pyridinium p-toluenesulfonate, (73 mg, 0.29 mmol) and tetraethoxy-silane (0.26 ml, 1.18 mmol) were suspended in 0.4 ml pyridine and stirred for 24 h at 20 °C. Afterwards Pd $[P(C_6H_6)_3]_4$ (70 mg, 0.06 mmol) and N,N-dicyclohexylmethylamine (0.35 ml, 2.06 mmol) were added and the reaction mixture was heated in a microwave oven to 160 °C for 20 min. The reaction mixture is diluted with 100 ml dichloromethan and extracted two times with 50 ml of a half saturated aqueous sodium hydrogencarbonat solution. The organic layer was dried with sodium sulfate, the solvent was evaporated under reduced pressure and the crude product was purified using chromatography method P3, yielding 190 mg (1.00 mmol) of 1*H*-Pyrrolo[3,2-*b*]pyridine-2-

Table 8
Chromatography methods.

	Column[a]	Solvent A	Solvent B	Flow rat [ml/min]	Gradient[b]
A1	Phenomenex, Mercury Gemini, C18, 3 μm, 2 × 20 mm, 40 °C	Water pH 8 (buffer: NH_3/NH_4HCO_3)	Acetonitril	1.0	5% → 95%, 2.5 min
P1	Waters, Sunfire, C18, 10 μm, 30 × 100 mm	Water with 0.2% formic acid	Acetonitril	100	10% → 65%, 6 min
P2	Waters, XBridge, C18, 10 μm, 30 × 100 mm	Water pH 8 (buffer: NH_3/NH_4CO_3)	Methanol	100	50% → 90%, 6 min
P2	Waters, XBridge, C18, 10 μm, 30 × 100 mm	Water pH 8 (buffer: NH_3/NH_4CO_3)	Methanol	100	10% → 75%, 6 min

[a] Company, column name, kind of particle, particle size, column dimension, column temperature.
[b] % of solvent B at gradient start → % of solvent B at gradient end, gradient time.

carboxylic acid ethyl ester. The ester was dissolved in 17 ml ethanol and 5 ml water. To this solution lithium hydroxide (120 mg, 5.00 mmol) was added. After 16 h the pH value of the reaction mixture was adjusted to pH 4 and the solvent is evaporated in vacuum. The crude product was purified using an acid ion exchanger (Strata-X-C, Phenomenex), yielding of 155 mg (82%) of the title compound. Purity by method A1: >95%; MS (ESI) *m/z* 163 $(M+H)^+$; ^{1}H NMR (DMSO) δ (ppm) 13.34 (br, 1H), 8.77 (d, $J = 5.3$ Hz, 1H), 8.53 (d, $J = 8.3$ Hz, 1H), 7.73 (dd, $J = 5.4$ Hz, $J = 8.3$ Hz, 1H), 7.33 (br, 1H); ^{13}C NMR (500 MHz, DMSO) δ (ppm) 161.4 (s), 138.0 (s), 136.1 (s), 135.8 (s), 132.7 (s), 128.6 (s), 119.6 (s), 101.2 (s).

*4.2.2.2. Acids **5g** and **5h**.* Pyrrolopyridine carboxylic acid **5g** and Indole carboxylic acid **5h** are synthesized in a similar manner to **5f**.

4.2.3. General method C – amide coupling

*4.2.3.1. (5-Chloro-7-fluoro-1H-indole-2-yl)-(4-methyl-piperazine-1-yl)-methanone (**49**).* (5-Chloro-7-fluoro-1*H*-indole-2-yl)-carboxylic acid **(5a)** (50 mg, 0.23 mmol), N,N-diisopropylethylamine (82 μl, 0.47 mmol) and 2-(7-Aza-1*H*-benzotriazole-1-yl)-1,1,3,3-tetramethyluronium hexafluorophosphate (89 mg, 0.23 mmol) were dissolved in 550 μl N,N-dimethylformamide. After stirring for 10 min 4-methyl-piperazin **6a** (26 μl, 0.23 mmol) was added and the reaction mixture was stirred for 16 h at 20 °C. The solvent was evaporated under reduced pressure and the crude product was purified using chromatography method P1, yielding 37 mg (53%) of the title compound. Purity by method A1: >95%; MS (ESI) *m/z* 296/298 $(M+H)^+$, Cl distribution; ^{1}H NMR (500 MHz, DMSO) δ (ppm) 12.32 (br, 1H), 7.55 (d, $J = 1.9$ Hz, 1H), 7.19 (dd, $J = 1.9$ Hz, $J_{HF} = 11.02$ Hz, 1H), 6.82 (d, $J = 3.1$ Hz, 1H), 3.68 (t, $J = 4.7$ Hz, 4H), 2.34 (t, $J = 4.7$ Hz, 4H), 2.21 (s, 3H); ^{13}C NMR (500 MHz, DMSO) δ (ppm) 161.2 (s), 148.7 (d, $J_{CF} = 249.1$ Hz), 133.1 (s), 130.7 (d, $J_{CF} = 6.4$ Hz), 123.3 (d, $J_{CF} = 8.5$ Hz), 122.7 (d, $J_{CF} = 13.1$ Hz), 116.6 (d, $J_{CF} = 3.6$ Hz), 108.5 (d, $J_{CF} = 20.2$ Hz), 103.8 (s), 54.6 (s), 46.6 (s).

4.2.3.2. Further amides. Amides **1**, **2a**, **10**–**19**, **21**, **23**, **26**, **28**, **30**–**32**, **34**, **36**, **38**, **39**, **40**, **42**, **43a**, **44a**, **45a**, **46**–**48**, **50**, **77**, **52a**, **53a**, **54a**, **55**–**63**, **64a**, **65a**, **66a**, **67**, **68a**, **69**–**71**, **72a**, **73a**, **74a**, **75**, **76** and **77** are synthesized in a similar manner to **49** – analytic data are given in the supplementary.

4.2.4. General method D – deprotection of boc group

*4.2.4.1. (7-Methyl-1H-indole-2-yl)-piperazine-1-yl-methanone (**43**).* 4-(7-Methyl-1*H*-indole-2-carbonyl)-piperazine-1-carboxylic acid *tert*-butyl ester **(43a)** (106 mg; 0.31 mmol) was dissolved in 2 ml dioxane and treated with a solution of HCl in dioxane (2 ml; 8 mmol). After the reaction mixture was stirred for 3 h at 20 °C, the solvent was evaporated in vacuum and the crude product was purified using method P2, yielding 39 mg (52%) of the title compound. Purity by method A1: >95%; MS (ESI) *m/z* 244 $(M+H)^+$; ^{1}H NMR (500 MHz, DMSO) δ (ppm) 11.39 (br, 1H), 7.42 (dd, $J = 1.9$ Hz, $J = 6.7$ Hz, 1H), 6.99–6.95 (m, 2H), 6.71 (d, $J = 1.9$ Hz, 1H), 3.68 (t, $J = 4.8$ Hz, 4H), 2.78 (t, $J = 4.8$ Hz, 4H), 2.49 (s, 3H); ^{13}C NMR (500 MHz, DMSO) δ (ppm) 162.4, 135.6, 130.2, 126.5, 123.4, 121.5, 120.0, 118.7, 104.0, 45.8, 17.1.

4.2.4.2. Further secondary amines. Free secondary amines **2**, **43**, **44**, **45**, **52**, **53**, **54**, **64**, **65**, **66**, **68**, **72**, **73** and **74** are synthesized in a similar manner to **43** – analytic data are given in the supplementary.

4.2.5. General method E – reduction of a nitro group

*4.2.5.1. 1(7-Amino-5-Chloro-1H-indole-2-yl)-(4-methyl-piperazine-1-yl)-methanone (**51**).* (5-Chloro-7-nitro-1*H*-indole-2-yl)-(4-methyl-piperazine-1-yl)methanone (**75**) (78 mg; 0.24 mmol) was dissolved in 20 ml methanol and 10 mg rany nickel was added. The reactor was charged with hydrogen gas and the reaction mixture was stirred for 2 h. The pressure in the reactor was always around 5 bar. Afterwards the catalyst was filtered of and washed three times with methanol. The solvent was evaporated under reduced pressure and the crude product was purified using method P2, yielding 68 mg (96%) of the title compound. Purity by method A1: >95%; MS (ESI) *m/z* 293/295 $(M+H)^+$, Cl distribution; ^{1}H NMR (500 MHz, DMSO) δ (ppm) 11.40 (br, 1H), 6.83 (d, $J = 1.7$ Hz, 1H), 6.68 (d, $J = 1.9$ Hz, 1H), 6.37 (d, $J = 1.7$ Hz, 1H), 5.66 (br, 2H), 3.75 (br, 4H), 2.34 (t, $J = 5.1$ Hz, 4H), 2.19 (s, 3H); ^{13}C NMR (500 MHz, DMSO) δ (ppm) 162.4, 135.6, 130.2, 126.5, 123.4, 121.5, 120.0, 118.7, 104.0, 45.8, 17.1.

4.2.5.2. Further anilines. Anilines **22**, **29**, **35** and **41** are synthesized in a similar manner to **51** – analytic data are given in the supplementary.

*4.2.6. 5-Chloro-7-nitro-1H-indole-2-carboxylic acid (**5c**)*

(4-Chloro-2-nitro-phenyl)hydrazine **4c** (3.55 g, 18.94 mmol), ethyl pyruvate **8** (2.10 ml, 18.94 mmol) and toluene-4-sulfonic acid monohydrate (84 mg, 0.44 mmol) were dissolved in 230 ml toluene and stirred for 1 h under reflux conditions and the resulting water was seperated through a water separator. The reaction mixture was cooled down to 20 °C and diluted with 300 ml ethyl acetate and treated with 100 ml of a half saturated aqueous sodium hydrogencarbonat solution. The organic layer was dried with sodium sulfate, the solvent was evaporated under reduced pressure, yielding 5.25 g (18.42 mmol) of 2-[(4-chloro-2-nitro-phenyl)-hydrazono]-propionic acid ethyl ester. The hydrazone (1.00 g, 3.50 mmol) was suspended in 10 g of polyphosphor acid at 100 °C. The reaction vessel with the suspension was put in pre heated oil bath at 195 °C for 5 min. The reaction mixture was cooled down to 50 °C and poured on 200 ml water and than treaded with sodium carbonate until pH 8 was reached. The mixture was 6 times extracted with 100 ml dichloromethane. The organic layer was dried with sodium sulfate, the solvent was evaporated under reduced pressure and the crude product was purified using chromatography method P2, yielding 390 mg (1.46 mmol) of 5-Chloro-7-nitro-1*H*-indole-2-carboxylic acid ethyl ester. The ester was dissolved in 10 ml ethanol and 10 ml water. To this solution lithium hydroxide (240 mg, 10.00 mmol) was added. After 16 h the pH value of the reaction mixture was adjusted to pH 4 and ethyl acetate was added. The organic layer was separated and dried with sodium sulfate. The solvent was evaporated under reduced pressure, yielding of 330 mg (95%) of the title compound. Purity by method A1: >95%; MS (ESI) *m/z* 163 $(M+H)^+$; ^{1}H NMR (DMSO) δ (ppm) 13.34 (br, 1H), 8.77 (d, $J = 5.3$ Hz, 1H), 8.53 (d, $J = 8.3$ Hz, 1H), 7.73 (dd, $J = 5.4$ Hz, $J = 8.3$ Hz, 1H), 7.33 (br, 1H); ^{13}C NMR (500 MHz, DMSO) δ (ppm) 161.8 (s), 134.0 (s), 133.5 (s), 132.1 (s), 129.6 (s), 127.8 (s), 123.7 (s), 120.8 (s), 107.9 (s).

4.2.7. General method F – ether cleavage

*4.2.7.1. (4-Hydroxy-1H-indole-2-yl)-(4-methyl-piperazine-1-yl)-methanone (**20**).* (4-Methoxy-1*H*-indole-2-yl)-(4-methyl-piperazine-1-yl)-methanone (**19**) (50 mg, 0.18 mmol) was dissolved in 1.5 ml dichloromethane and treated with a boron-tribromide solution (0.65 ml, 0.65 mmol). The resulting yellow suspension was stirred for 4 h. Afterwards the solvent was evaporated under reduced pressure and the crude product was purified using method P3, yielding 11 mg (23%) of the title compound. Purity by method A1: >95%; MS (ESI) *m/z* 260 $(M+H)^+$; ^{1}H NMR (500 MHz, DMSO) δ (ppm) 11.44 (br, 1H), 9.58 (s, 1H), 7.01 (dd, $J = 7.9$ Hz, $J = 8.3$ Hz, 1H), 6.90 (d, $J = 8.3$ Hz, 1H), 6.86 (d, $J = 1.7$ Hz, 1H), 6.41 (d, $J = 7.8$ Hz, 1H), 3.79 (br, 4H), 2.39 (t, $J = 4.9$ Hz, 4H), 2.24 (s, 3H); ^{13}C

NMR (500 MHz, DMSO) δ (ppm) 161.8, 151.2, 137.7, 127.9, 124.3, 117.4, 103.3, 103.2, 101.6, 54.8, 45.7.

4.2.7.2. Additional phenol. Phenol **33** is synthesized in a similar manner to **20** – analytic data are given in the supplementary.

Appendix A. Supplementary data

Supplementary data associated with this article can be found in the online version, at doi:10.1016/j.ejmech.2012.06.016. These data include MOL files and InChiKeys of the most important compounds described in this article.

References

[1] C. Liu, X.-J. Ma, X. Jiang, S.J. Wilson, C.L. Hofstra, K. Blevitt, J. Pyati, X. Li, W. Chai, N. Carruthers, T.W. Lovenberg, Cloning and pharmacological characterization of a fourth histamine receptor (H4) expressed in bone marrow, Mol. Pharmacol. 59 (2001) 420–426.

[2] T. Nguyen, D.A. Shapiro, S.R. George, V. Setola, D.K. Lee, R. Cheng, L. Rauser, S.P. Lee, K.R. Lynch, B.L. Roth, B.F. O'Dowd, Discovery of a novel member of the histamine receptor family, Mol. Pharmacol. 59 (2001) 427–433.

[3] Y. Zhu, D. Michalovich, H.-L. Wu, K.B. Tan, G.M. Dytko, I.J. Mannan, R. Boyce, J. Alston, L.A. Tierney, X. Li, N.C. Herrity, Cloning, expression and pharmacological characterization of a novel human histamine receptor, Mol. Pharmacol. 59 (2001) 434–441.

[4] M. Zhang, R.L. Thurmond, P.J. Dunford, The histamine H4 receptor: a novel modulator of inflammatory and immune disorders, Pharmacol. Ther. 113 (2007) 594–606.

[5] B.B. Damaj, C.B. Becerra, H.J. Esber, Y. Wen, A.A. Maghazachi, Functional expression of H4 histamine receptor in human natural killer cells, monocytes, and dendritic cells, J. Immunol. 179 (2007) 7907–7915.

[6] M.I. Strakhova, A.L. Nikkel, A.M. Manelli, G.C. Hsieh, T.A. Esbenshade, J.D. Brioni, R.S. Bitner, Localization of histamine H4 receptors in the central nervous system of human and rat, Brain Res. 1250 (2009) 41–48.

[7] W.M. Connelly, F.C. Shenton, N. Lethbridge, R. Leurs, H.J. Waldvolgel, R.L. Faull, G. Lees, P.L. Chazot, The histamine H4 receptor is functionally expressed on neurons in the mammalian CNS, Br. J. Pharmacol. 157 (2009) 55–63.

[8] P.J. Dunford, K.N. Williams, P.J. Desai, D. McQueen, L. Karlsson, R. Thurmond, Histamine H4 receptor antagonists are superior to traditional antihistamines in the attenuation of experimental pruritus, J. Allergy Clin. Immunol. 119 (2007) 176–183.

[9] J. Rees, C.S. Murray, Itching for progress, Clin. Exp. Dermatol. 30 (2005) 471–473.

[10] R.L. Thurmond, E.W. Gelfand, P.J. Dunford, The role of histamine H1 and H4 receptors in allergic inflammation: the search for new antihistamines, Nat. Rev. Drug Discovery 7 (2008) 41–53.

[11] P. Ling, K. Ngo, S. Nguyen, R.L. Thurmond, J.P. Edwards, L. Karlsson, W.P. Fung-Leung, Histamine H4 receptor mediates eosinophil chemotaxis with cell shape change and adhesion molecule upregulation, Br. J. Pharmacol. 142 (2004) 161–171.

[12] K.F. Buckland, T.J. Williams, D.M. Conroy, Histamine induces cytoskeletal changes in human eosinophils via the H4 receptor, Br. J. Pharmacol. 140 (2003) 1117–1127.

[13] C.A. Akdis, F. Simons, R. Estelle, Histamine receptors are hot in immunopharmacology, Eur. J. Pharmacol. 533 (2006) 69–76.

[14] J.A. Jablonowski, C.A. Grice, W. Chai, C.A. Dvorak, J.D. Venable, A.K. Kwok, K.S. Ly, J. Wei, S.M. Baker, P.J. Desai, W. Jiang, S.J. Wilson, R.L. Thurmond, L. Karlsson, J.P. Edwards, T.W. Lovenberg, N.I. Carruthers, The first potent and selective non-imidazole human histamine H4 receptor antagonists, J. Med. Chem. 46 (2003) 3957–3960.

[15] J.D. Venable, H. Cai, W. Chai, C.A. Dvorak, C.A. Grice, J.A. Jablonowski, C.R. Shah, A.K. Kwok, K.S. Ly, B. Pio, J. Wie, P.J. Desai, W. Jiang, S. Nguyen, P. Ling, S.J. Wilson, P.J. Dunford, R.L. Thurmond, T.W. Lovenberg, L. Karlsson, N.I. Carruthers, J.P. Edwards, Preparation and biological evaluation of indole, benzimidazole, and thienopyrrole piperazine carboxamides: potent human histamine H4 antagonists, J. Med. Chem. 48 (2005) 8289–8298.

[16] J. Edwards, B. Savall, C. R. Shah. PCT Pat. Appl. WO 20071117401, March 30, 2007.

[17] E.P. Istyastono, S. Nijmeijer, H.D. Lim, A. van de Stolpe, L. Roumen, A.J. Kooistra, H.F. Vischer, I.J.P. de Esch, R. Leurs, C. de Graaf, Molecular determinants of ligand binding modes in the histamine H 4 receptor: linking ligand-based three-dimensional quantitative structure–activity relationship (3D-QSAR) models to in silico guided receptor mutagenesis studies, J. Med. Chem. 54 (2011) 8136–8147.

[18] R.A. Smits, H.D. Lim, B. Stegink, R.A. Bakker, I.J.P. de Esch, R. Leurs, Characterization of the histamine H4 receptor binding site. Part 1. Synthesis and pharmacological evaluation of dibenzodiazepine derivatives, J. Med. Chem. 49 (2006) 4512–4516.

[19] R.A. Smits, I.J.P. de Esch, O.P. Zuidervel, J. Broeker, K. Sansuk, E. Guaita, G. Coruzzi, M. Adami, E. Haaksma, R. Leurs, The discovery of quinazolines as histamine H_4 receptor inverse agonists using a scaffold hopping approach, J. Med. Chem. 51 (2008) 7855–7865.

[20] M.D. Cowart, R.J. Altenbach, H. Liu, G.C. Hsieh, I. Drizin, I. Milicic, T.R. Miller, D.G. Witte, N. Wishart, S.R. Fix-Stenzel, M.J. McPherson, Rotationally constrained 2,4-diamino-5,6-disubstituted pyrimidines: a new class of histamine H4 receptor antagonists with improved druglikeness and in vivo efficacy in pain and inflammation models, J Med. Chem. 51 (2008) 6547–6557.

[21] R.J. Altenbach, R.M. Adair, B.M. Bettencourt, L.A. Black, S.R. Fix-Stenzel, S.M. Gopalakrishnan, G.C. Hsieh, H. Liu, K.C. Marsh, M.J. McPherson, I. Milicic, T.R. Miller, T.A. Vortherms, U. Warrior, J.M. Wetter, N. Wishart, D.G. Witte, P. Honore, T.A. Esbenshade, A.A. Hancock, J.D. Brioni, M.D. Cowart, Structure-activity studies on a series of a 2-aminopyrimidine-containing histamine H_4 receptor ligands, J. Med. Chem. 51 (2008) 6571–6580.

[22] H. Engelhardt, R.A. Smits, R. Leurs, E. Haaksma, I.J.P. de Esch, A new generation of anti-histamines: histamine H4 receptor antagonists on their way to the clinic, Curr. Opin. Drug Disc. Dev. 12 (2009) 628–643.

[23] R. Kiss, G.M. Keserú, Histamine H4 receptor ligands and their potential therapeutic applications, Expert Opinion 19 (2009) 119–135.

[24] R. Kiss, B. Kiss, A. Könczöl, F. Szalai, I. Jelinek, V. László, B. Noszál, A. Falus, G.M. Keserú, J. Med. Chem. 51 (2008) 3145–3153.

[25] S.M. Free, J.W. Wilson, A mathematical contribution to structure- activity studies, J. Med. Chem. 7 (1964) 395–399.

[26] K. Sugano, T. Kato, K. Suzuki, K. Keiko, T. Sujaku, T. Mano, High throughput solubility measurement with automated polarized light microscopy analysis, J. Pharm. Sci. 95 (2006) 2115–2122.

[27] S.M. Skaggs, R.S. Foti, M.B. Fischer, A streamlined method to predict hepatic clearance using human liver microsomes in the presence of human plasma, J. Pharmacol. Toxicol. Method. 53 (2006) 284–290.

[28] R Development Core Team, R: A Language And Environment for Statistical Computing, R Foundation for Statistical Computing, Vienna Austria, 2009, ISBN 3-900051-07-0, URL, http://www.R-project.org.

[29] Pipeline Pilot, version 7.5; Accelrys Software Inc.: San Diego.